Bioorganic Chemistry 54 (2014) 81–88

Contents lists available at ScienceDirect

Bioorganic Chemistry

journal homepage: www.elsevier.com/locate/bioorg

3-Hydroxypyrrolidine and (3,4)-dihydroxypyrrolidine derivatives: Inhibition of rat intestinal α-glucosidase

Elisabete P. Carreiro [b], Patrícia Louro [a,c], Gizé Adriano [a,b], Romina A. Guedes [c], Nicholas Vannuchi [c], Ana R. Costa [a,c], Célia M.M. Antunes [a,c,e], Rita C. Guedes [d], A.J. Burke [a,*]

[a] Departamento de Química, Universidade de Evora, Rua Romão Ramalho, 59, 7000 Evora, Portugal
[b] Centro de Química de Évora, Rua Romão Ramalho, 59, 7000 Évora, Portugal
[c] Instituto de Ciências Agrárias e Ambientais Mediterrânicas (ICCAM), Apartado 94, 7002-554, Universidade de Évora, Portugal
[d] Instituto de Investigação do Medicamento (iMed.ULisboa), Faculty of Pharmacy, Universidade de Lisboa, Av. Prof. Gama Pinto, 1649-003 Lisbon, Portugal
[e] Center For Neurosciences and Cell Biology, University of Coimbra, Portugal

ARTICLE INFO

Article history:
Received 20 February 2014
Available online 30 April 2014

Keywords:
1-Benzyl-3-hydroxypyrrolidine
1-Benzyl-3,4-dihydroxypyrrolidine
Small molecule inhibitor
α-Glucosidase
Rat intestinal cells

ABSTRACT

Thirteen pyrrolidine-based iminosugar derivatives have been synthesized and evaluated for inhibition of α-glucosidase from rat intestine. The compounds studied were the non-hydroxy, mono-hydroxy and dihydroxypyrrolidines. All the compounds were *N*-benzylated apart from one. Four of the compounds had a carbonyl group in the 2,5-position of the pyrrolidine ring. The most promising iminosugar was the *trans*-3,4-dihydroxypyrrolidine 5 giving an IC_{50} of 2.97 ± 0.046 and a K_I of 1.18 mM. Kinetic studies showed that the inhibition was of the mixed type, but predominantly competitive for all the compounds tested. Toxicological assay results showed that the compounds have low toxicity. Docking studies showed that all the compounds occupy the same region as the DNJ inhibitor on the enzyme binding site with the most active compounds establishing similar interactions with key residues. Our studies suggest that a rotation of ~90° of some compounds inside the binding pocket is responsible for the complete loss of inhibitory activity.

Despite the fact that activity was found only in the mM range, these compounds have served as simple molecular tools for probing the structural features of the enzyme, so that inhibition can be improved in further studies.

1. Introduction

Over the last two decades, glycosidase inhibitors have been a key target for academic researchers, because of their role in a variety of ailments [1], such as: diabetes mellitus type II [2], cancer [3], hepatitis [4], HIV [5] and Gaucher disease [6]. One of the most studied classes of inhibitor are the polyhydroxylated pyrrolidines and piperidines [7]. Before the 90s [8] most glycosidase inhibitors studied were obtained from plants and micro-organisms, and three important examples are: deoxynojirimycin (**DNJ**), 2*R*,5*R*-dihydroxymethyl-3*R*,4*R*-dihydroxypyrrolidine (**DMDP**) and 1,4-dideoxy-1,4-imino-D-arabinitol (**DAB**) (Fig. 1). These three molecules have been the prototypes for the synthesis of a wide range of potential glycosidase inhibitors [1]. For example, miglitol, an *N*-alkyl derivative of **DNJ** used in the treatment of diabetes [2]. Curiously, Miglustat (*N*-butyl **DNJ**, Zavesca) is structurally similar to miglitol and is licensed for substrate reduction therapy in Gaucher's disease. In the case of **DAB**, it shows strong inhibition of α-glucosidases, but its enantiomer, **LAB** is more potent and specific than **DAB** [9]. In the literature there exists an extensive variety of iminosugars with structures based on the pyrrolidine unit, which exhibit α-glucosidase activity. Several derivatives of **DAB** were synthesized and tested in different types of α-glucosidases [10]. Most of the structures were functionalized with alkyl [11], aryl [12], amide [13], amine [13], or hydroxyl [14] units in the 2,5-positions of the pyrrolidine ring. In 2012 Kato et al. [11a] described a new family of potent pyrrolidine α-glucosidase inhibitors; this family was basically a set of analogues of the **LAB** structure, having alkyl chains of different lengths in the 2 and 4 positions. The most promising α-glucosidase inhibitor was the 1-C butyl derivative, which is one order of magnitude more active than **LAB** (Fig. 1). On the contrary, the 2,4 dibutyl derivative did not show any inhibition, leading us to conclude that the hydroxyl group in the 4-postion is important for α-glucosidase inhibition.

Recently we designed and synthesized a small library of pyrrolidine iminocyclitol inhibitors with a structural similarity to **DAB**.

* Corresponding author.
E-mail address: ajb@uevora.pt (A.J. Burke).

http://dx.doi.org/10.1016/j.bioorg.2014.04.007
0045-2068/

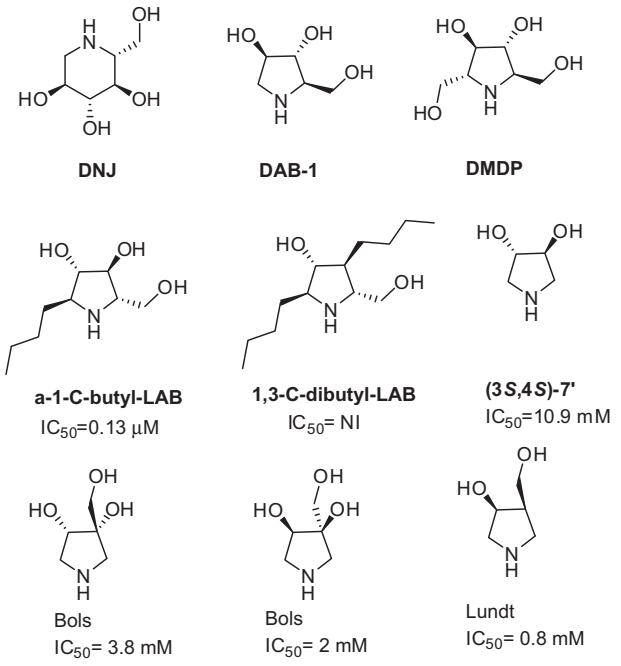

Fig. 1. Examples of natural and synthetic iminosugars. NI = No inhibition.

This library was specifically designed to gain a better insight into the mechanism of inhibition of glycosidases by polyhydroxylated pyrrolidines. These compounds were assayed for baker's yeast α-glucosidadse inhibition using acarbose as a reference and it was the non-benzylated diol **7′** which showed the highest inhibition (IC_{50} = 10.9 mM). It seems that the presence of a free NH group and free hydroxyl groups in the 3 and 4 positions are important for favorable interaction with the enzyme active site. There were no substituents in the 2,5-position of the pyrrolidine ring in these compounds, but it appears quite obvious that the presence of substituents in these positions is important for inhibition [7]. Our results are similar to those obtained with the iminosugars reported by Bols [15] and Lundt [16] (Fig. 1), although in their case the 3,4-hydroxy groups had a *cis* relative configuration.

In this publication we report a study of another library of 1-benzyl-3-hydroxypyrrolidine derivatives (**1**, **1′**, **2**, **2′**, **3**, **3′**, **4**, **4′**) and 1-benzyl-3,4-dihydroxypyrrolidne derivatives (**5**, **5′**, **6**, **7**), derived from D- and L-malic acid and D- and L-tartaric acid (Fig. 2),

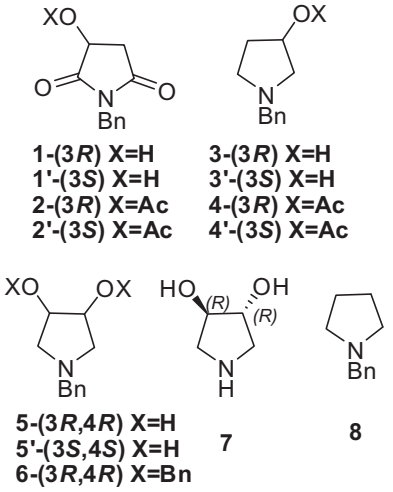

Fig. 2. Library of 5-membered iminosugars synthesized and tested.

respectively. It must be noted that a wide range of important pharmacologically active compounds contain the 3-hydroxypyrrolidine subunit, one example is *Barnidipine*, an antihypertensive agent [17]. In our study, the compounds were assayed for rat intestine α-glucosidase (EC 3.2.1.20) [18] inhibition, as well as the mechanism of inhibition and K_I determination. Acarbose and DNJ were used as references. Cytoxicity studies were also conducted for compounds **5**, **5′** and **7**. Docking studies were realized with the human α-glucosidase (intestinal maltase-glucoamylase) and a homology model of rat glucosidase. We wanted to compare both the monohydroxypyrrolidine and dihydroxypyrrolidine series with pyrrolidines lacking an hydroxyl group. The structural diversity encountered in this library was for the purpose of probing the mechanism of inhibition of α-glycosidase, so that we can design and synthesize more potent, non-toxic α-glycosidase inhibitors. On the basis of our last publication we observed that *O*-acetylated dihydroxypyrrolidines – despite showing good docking simulations [7a] – seem to suffer hydrolysis during the biological assays, and for this reason we decided to substitute the acetyl group for the more robust benzyl group. Besides this, the possibility of the benzyl groups establishing significant non-covalent π–π interactions with the active site residues was very likely, and worth investigating.

2. Materials and methods

2.1. General chemical

All reagents were obtained from Aldrich, Fluka, Alfa Aesar or Acros. Solvents were dried using common laboratory methods. Compounds **5** and its respective enantiomer **5′** were synthesized using the precursors: (3*S*,4*S*)-*N*-benzyl-3,4-dihydroxy-2,5-dioxopyrrolidine and (3*R*,4*R*)-*N*-benzyl-3,4-dihydroxy-2,5-dioxopyrrolidine, respectively, both enantiomers had an enantiomeric purity of 99% ee. TLC was carried out on aluminum backed Kiselgel 60 F_{254} plates (Merck) and the plates were visualized either by UV light or with phosphomolybdic acid in ethanol. The ^{1}H NMR and ^{13}C NMR spectra were recorded on a Bruker Avance instrument (^{1}H: 400 MHz and ^{13}C: 100 MHz) using $CDCl_3$ as solvent and the signal from residual $CHCl_3$ as an internal standard (for the measurements made with the Bruker Avance instrument). Specific rotations were measured on a Perkin–Elmer 241 polarimeter.

2.2. General biological assays

2.2.1. Enzymatic assays with rat α-glucosidase

The enterocytes were isolated from *Wistar* rat small intestine according to Watford et al. [19a] with some modifications. The α-glucosidase rich homogenates were obtained after mucus removal with calcium free Krebs-Henseilt buffer (in mM: 120 NaCl, 2 KCl, 26 $NaHCO_3$, 10 $MgSO_4$, 1.18 KH_2PO_4, 11 glucose, 5 EDTA; supplemented with 0.25% (p/v) BSA; at 37 °C during 20 min under mild stirring – 60 rpm) and detachment of mucosa epithelial cells using Krebs-Henseilt buffer (as previously described without EDTA and with 0.5 mM $CaCl_2$, supplemented with 2.5% (p/v) BSA). The total protein concentration was determined using the Bradford dye-binding method [19b].

The α-glucosidase activity was determined by monitoring the *p*-nitrophenol (*p*-NP) released from *p*-nitrophenyl-α-D-glycopyranoside spectrophotometrically at 405 nm, over 60 min. The assay mixture had the following composition: 0.1 M phosphate buffer (pH 6.7), 12 mM *p*-nitrophenyl-α-D-glucopyranoside (the method was optimized giving K_M and V_{max} values of 0.961 mM and 2.51×10^{-5} mmol *p*-NP min^{-1} mg^{-1}, respectively) and 30 μg/mL rat enterocyte α-glucosidase rich homogenates. The test compounds were dissolved in 2% DMSO in 0.1 M phosphate buffer

(pH 7) and solutions with concentration in the range of 0.01×10^{-3} and 92 mM were used. All experiments were performed in 5 replicates. The IC_{50} values were obtained from the inhibition curves.

2.2.2. Toxicity assays

The toxicity of the compounds was measured using two methods. The first method consisted of the determination of the cell viability of the cellular line BRIN-BD 11 from pancreatic beta cells. The second method entailed the evaluation of the half maximal lethal concentration (LC_{50}) using *Artemia salina*.

2.2.2.1. Cytotoxicity assay. BRIN BD-11 cells were cultured in 96 well micro plates (2×10^4 cells/well) in an incubator at 37 °C with 5% CO_2 and 95% O_2. The cells were exposed to the test compounds in the concentration range of 3–50 mM for 24 h. A negative control (without inhibitors) and a positive control (1% sodium dodecyl sulfate) tests were performed. Cell viability was determined using the *cell counting kit-8* (CCK-8, Sigma–Aldrich) as established by the supplier.

2.2.2.2. Artemia salina lethal toxicity assay. The percentage of dyed nauplii of *Artemia salina*, grown in the presence of variable concentrations of the inhibitor compounds, was measured to determine the LC_{50} values. The Artoxkit M was used.

2.2.3. Statistical analysis

Results are presented as mean ± sd for a given number of observations. Statistical analyses were done using one-way ANOVA for enzymatic activity. In the case of the toxicological results *Paired-samples t-Test* was used for comparison with samples showing negative control.

2.3. Molecular modeling

2.3.1. Molecular docking calculations

Molecular docking calculations of the synthesized compounds with human and a homology model of rat α-glucosidase were performed with GOLD 5.1.0 (Genetic Optimization Ligand Docking) [20] software using the Goldscore scoring function. This software uses an evolutionary genetic algorithm to optimize the docked conformation of the flexible inhibitor within the enzyme. The docking calculations were performed using the homology model described in the next section for the rat α-glucosidase and the available human α-glucosidase crystallographic structure. The experimental X-ray structure was obtained from the RCSB Protein Data Bank (PDB ID 3L4U, resolution 1.9 Å). The preparation of the human α-glucosidase structure involved the removal of the original crystallographic ligand (kotalanol) as well as the crystallographic waters. The protonation and tautomeric states of Asp, Glu, Arg, Lys, and His were adjusted to match a pH of 7 using the Protonate 3D algorithm within the Molecular Operating Environment (MOE) 2012.10 program (www.chemcomp.com). These enzyme structures and the proposed docking protocol were previously validated by re-docking the co-crystallized ligand. The molecular structures of the synthesized compounds were built and optimized with MOE package (2012.10) with the MMFF94x forcefield as implemented in this software. These compounds were docked into the homology model of rat intestinal glucosidase and to human glucosidase active sites. For each compound, 500 docking runs were performed. The following genetic algorithm parameters were used: population size = 100; selected pressure = 1.1; number of operations = 1000; number of islands = 5; niche size = 2; migrate = 10; mutate = 95; crossover = 95. Each conformation was ranked according to its goldscore scoring function. The top solutions (the ones with the highest goldscore) were visually inspected and critically evaluated and, for each inhibitor, the highest scoring conformation was chosen as the actual binding conformation (Fig. 3).

2.4. Homology modeling of the rat intestinal glucosidase

To investigate the inhibitory activity of the synthesized compounds against rat intestinal glucosidase, a homology modeling of α-glucosidase from *Rattus norvegicus* was carried out to predict its 3D-structure (the 3D structure has never been resolved experimentally). The amino acid sequence of α-glucosidase from *Rattus norvegicus* comprises 953 amino acid residues and was retrieved from the UniProt protein resource data bank (http://www.uniprot.org/), under the access code Q6P7A9. Using the Molecular Operating Environment program (MOE) version 2012.10 (http://www.chemcomp.com/software) we searched for proper structural templates on the PDB database of protein structures and sequences and aligned the results obtained with the MOE-Align feature. MOE-Align implement a modified version of the alignment methodology originally introduced by Needleman and Wunsch. All the default settings in the MOE-Align panel were used for the sequence alignment. Our search identified the *Homo sapiens* intestinal maltase-glucoamylase (in complex with O-sulfonated kotalanol) crystallographic structure (PDB code 3L4U, 1.90 Å resolution) [21] sharing 45.7% of sequence identity (calculated with BLAST) with α-glucosidase enzyme from *Rattus norvegicus* as the most suitable template. The catalytic site is highly conserved in both structures. The crystallographic structure and the homology model were superimposed with MOE software and the RMSD values obtained were 1.04 Å for the *Rattus norvegicus* homology model. The 3D homology models were built with Molecular Operating Environment (MOE) software using only a single template and a set of 10 intermediate models were generated and refined with Amber99 forcefield, resulting in the corresponding homology model. The stereochemical quality of the enzyme backbone and side chains was validated by Ramachandran plots. To validate the model we first docked kotanalol into the structure's active site and compared the final docked complexes with the crystallographic structure obtained by Sim et al. [21]. We confirmed that kotanalol was placed in an identical position to that adopted in the crystallographic structure (PDB ID: 3L4U) having similar active site residue interactions.

Besides that, acarbose (a known α-glucosidase inhibitor widely used in the treatment of diabetes type 2) was also docked into the homology model active site, and was correctly positioned.

2.5. Synthesis of pyrrolidine iminocyclitol inhibitors

Synthesis of (3*R*)-1-benzyl-3-hydroxypyrrolidine-2,5-dione (1): (3*R*)-1-benzyl-3-pyrrolidine-2,5-dione **1** was synthesized according to the thermal condensation method [22a,23]. The enantioselectivity was determined by chiral HPLC (column AD-H, (60:40) n-hexane:ethanol, 1 mL/min) t_R = 15.8 min, 98% ee.

Synthesis of (3*S*)-1-benzyl-3-hydroxypyrrolidine-2,5-dione (1′): (3*S*)-1-benzyl-3-hydroxypyrrolidine-2,5-dione **1′** was synthesized according to the thermal condensation method [22a,23]. The enantioselectivity was determined by chiral HPLC (AD-H, (60:40) n-hexane:ethanol, 1 mL/min: t_R = 20.6 min, 100% ee.

Synthesis of (3*R*)-1-benzyl-3-acetatoxypyrrolidine-2,5-dione (2): (3*R*)-1-benzyl-3-hydroxypyrrolidine-2,5-dione **1** (300 mg, 1.5 mmol) was dissolved in pyridine (0.78 mL) and acetic anhydride (1.23 mL) was then added. The solution was stirred for 23 h at rt. The solvents were removed *in vacuo*, and the crude product was purified by silica gel column chromatography [(2:1) to (1:1) Hex:EtOAc)] to give the *title compound* as a light brown solid (0.19 g, 52%).

^{1}H NMR ($CDCl_3$, 400 MHz) δ: 2.14 (s, 3H, CH_3) ppm, 2.64 (dd, *J* 4, 20 Hz, 1H, CH_2CO), 3.13 (dd, *J* 8, 20 Hz, 1H, CH_2CO), 4.6 (d, *J* 20 Hz,

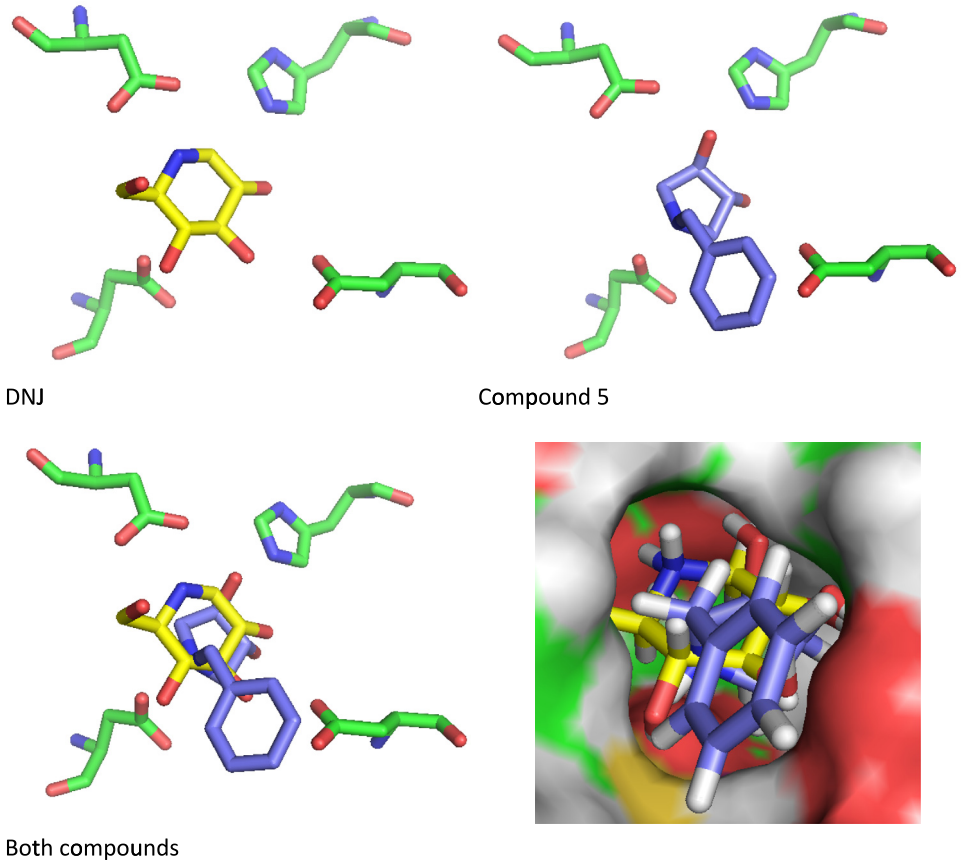

Fig. 3. Docking poses of DNJ and compound **5** inside the human α-glucosidase active site.

1H, ABX system, CH_2Ph), 4.7(d, *J* 12,1H, ABX system, CH_2Ph), 5.42 (dd, *J* 8, 12 Hz, 1H, CHOAc), 7.33 (m, 5H, Ph). ^{13}C NMR (100.6 MHz, $CDCl_3$): δ = 20.5 ppm, 35.7, 42.6, 67.5, 128.1, 128.7, 128.9, 135.1, 169.8, 172.9, 173.2. $[\alpha]_D^{28}$ = +20.6 (*c* 1.45, $CHCl_3$). {$[\alpha]_D^{20}$ = +39 (1%, w/v MeOH)} [24].

Synthesis of (3*S*)-1-benzyl-3-acetatoxypyrrolidine-2,5-dione (2′): (3*S*)-1-benzyl-3-acetatoxypyrrolidine-2,5-dione **2′** was synthesized according the procedure described previously, the *title compound* was obtained as a brown solid (0.29 g, 78%).

^1H NMR (400 MHz, $CDCl_3$): δ 2.14 (s, 3H, CH_3) ppm, 2.64 (dd, *J* = 4, 16 Hz, 1H, CH_2CO), 3.14 (dd, *J* 8, 20 Hz, 1H, CH_2CO), 4.65 (d, *J* 16 Hz, 1H, ABX system, CH_2Ph), 4.70 (d, *J* 16 Hz, 1H, ABX system, CH_2Ph), 5.25 (dd, *J* 4, 8 Hz, 1H, CHOAc), 7.34 (m, 5H, Ph). ^{13}C NMR (100.6 MHz, $CDCl_3$): δ 20.5 ppm, 35.7, 42.7, 67.5, 128.2, 128.7, 128.9, 135.2, 169.8, 172.9, 173.2. $[\alpha]_D^{28}$ = −21.5 (*c* 1.14, $CHCl_3$). {$[\alpha]_D^{20}$ = −40.6 (1%, w/v MeOH)} [22].

Synthesis of (3*R*)-1-benzyl-3-hydroxypyrrolidine (3): (3*R*)-1-benzyl-3-hydroxypyrrolidine **3** was synthesized according to the method described by Zheng et al. [22a] $[\alpha]_D^{29}$ = +56.3 (*c* 0.045, $CHCl_3$).

Synthesis of (3*S*)-1-benzyl-3-hydroxypyrrolidine (3′): (3*S*)-1-benzyl-3-hydroxypyrrolidine-2,5 **3′** was synthesized according to the method described by Zheng et al. [22a] $[\alpha]_D^{29}$ = −3.14 (*c* 1.08, $CHCl_3$). {$[\alpha]_D^{25}$ = −3.145 (*c* 1.2, $CHCl_3$)} [22a].

Synthesis of (3*R*)-1-benzyl-3-acetatepyrrolidine (4): (3*R*)-1-benzyl-3-acetatoxypyrrolidine **4** was synthesized according to the method described for compound **2**, the *title compound* was obtained as a brown solid (0.14 g, 63%).

^1H NMR (400 MHz, $CDCl_3$): δ 1.85 (m, 1H, CH_2) ppm, 2.03 (s, 3H, CH_3), 2.25 (m,1H, CH_2), 2.46 (m, 1H, CH_2), 2.66 (m, 1H, CH_2), 2.8 (m, 2H, CH_2), 3.60 (d, *J* 12 Hz, 1H, ABX system, CH_2Ph), 3.7(d, *J* 12 Hz, 1H, ABX system, CH_2Ph), 5.17 (m, 1H, CHOAc), 7.28 (m, 5H, Ph); ^{13}C NMR (100.6 MHz, $CDCl_3$): δ 21.0 ppm, 31.6, 52.5, 59.7, 60.1, 74.1, 127.6, 128.7, 129.4, 138.6, 171.0. $[\alpha]_D^{28}$ = +5.01 (*c* 3.77, $CHCl_3$). {$[\alpha]_D$ = +22.0 (*c* 5, MeOH)} [25].

Synthesis of (3*S*)-1-benzyl-3-acetatepyrrolidine (4′): (3*S*)-1-benzyl-3-acetatoxypyrrolidine **4′** was synthesized according to the method described for compound **2**, the *title compound* was obtained as a brown solid (0.11 g, 49%).

^1H NMR (400 MHz, $CDCl_3$): δ 1.86 (m, 1H, CH_2) ppm, 2.04 (s, 3H, CH_3), 2.27 (m,1H, CH_2), 2.40 (m, 1H, CH_2, 2.66 (m, 1H, CH_2), 2.78 (m, 2H, CHH), 3.60 (d, *J* 12 Hz, 1H, ABX system, CH_2Ph), 3.69 (d, *J* 16 Hz, 1H, ABX system, CH_2Ph), 5.18 (m, 1H, CHOAc), 7.29 (m, 5H, Ph); ^{13}C NMR (100.6 MHz, $CDCl_3$): δ 21.3 ppm, 31.9, 52.7, 59.9, 60.2, 74.1, 127.6, 128.3, 128.9, 138.5, 171.0. $[\alpha]_D^{28}$ = −19 (*c* 2.4, $CHCl_3$). {$[\alpha]_D^{20}$ = −23.0 (*c* 1, MeOH)} [26].

Synthesis of (3*R*,4*R*)-1-benzyl-3,4-dihydroxypyrrolidine (5): (3*R*,4*R*)-1-benzyl-3-dihydroxypyrrolidine **5** was synthesized according to the method of Nagel [23]. $[\alpha]_D^{20}$ = −30.5 (*c* 4.23, MeOH).

Synthesis of (3*S*,4*S*)-1-benzyl-3,4-dihydroxypyrrolidine (5′): (3*S*,4*S*)-1-benzyl-3-dihydroxypyrrolidine **5′** was synthesized according to the method of Nagel [23]. $[\alpha]_D^{20}$ = +40 (*c* 3.7, MeOH) [$[\alpha]_D^{20}$ = +32.4 (*c* 4.2, MeOH)] [23a].

Synthesis of (3*R*,4*R*)-1-benzyl-3,4-bis(benzyloxy)pyrrolidine (6): NaH (0.828 g; 60% dispersion in mineral oil, 21 mmol) was added to a suspension of (3*R*,4*R*)-1-benzyl-3,4-pyrrolidinediol **5** (1 g, 5.2 mmol) in anhydrous DMF (2 mL) at room temperature. The suspension was stirred for 3 min then cooled in an ice bath. Benzyl bromide (1.85 mL, 16 mmol) was added dropwise over a 5-min period, and after 1 min the ice bath was removed. The reaction mixture was stirred overnight, and then 1 mL of MeOH was added slowly to react with the excess of the NaH. DMF was removed under reduced pressure at 55 °C. The residue was

dissolved in CH_2Cl_2 (25 mL) and washed with water and brine, dried ($MgSO_4$), filtered, and evaporated to give the crude product **6** as a yellow oil which was purified by silica gel column chromatography [hexane, to (9:1) hexane:EtOAc to EtOAc] (1.16 g, 60%, as a colorless oil).

^{1}H NMR (400 MHz, $CDCl_3$): δ 2.74 ppm (dd, *J* 4, 8 Hz, 2H, CH_2), 2.99 (dd, *J* 4, 12 Hz, 2H, CH_2), 3.66 (d, *J* 12 Hz, 1H, ABX system, CH_2), 3.73(d, *J* 12 Hz, 1H, ABX system, CH_2), 4.16 (d, 2H, 2xCH), 4.57 (q, 4H, 2x CH_2Ph), 7.37 (m, 15H, Ph). ^{13}C NMR (100 MHz, $CDCl_3$): δ 58.5 ppm, 60.4, 71.5, 83.7, 127.1, 127.7, 127.9, 128.3, 128.4, 129.0, 138.2, 138.4. $[\alpha]_D^{28} = -28.6$ (*c* 1.13, $CHCl_3$). MS (ESI-TOF) 374.22 (M + 1).

2.5.1. (3R,4R)-pyrrolidine-3,4-diol (7)

A dry 5 mL round-bottomed flask containing a magnetic stirring bar was charged with (3*R*,4*R*)-1-benzyl-3,4-dihydroxypyrrolidine diol **5** (0.45 g, 2.3 mmol), EtOH (15 mL) and Pd(0)En cat 3NP (1 g, 0.4 mmol Pd/g). A balloon filled with hydrogen was attached to the flask, the mixture was warmed to 50 °C and stirred for 26 h. It was then allowed to cool to room temperature, filtered and washed with CH_2Cl_2 (3 mL), and the solvent was removed *in vacuo* giving **7** (0.24 g, 100%) as a white solid.

^{1}H NMR (400 MHz, D_2O): δ 3.36 ppm (d, *J* 12 Hz, CHH, 2H), 3.6 (d, *J* 12 Hz, CHH, 2H), 4.41 (s, 2H, CHO, 2H). ^{13}C NMR (D_2O, 100 MHz): δ 49.2 ppm, 72.7.

2.5.2. 1-Benzyl pyrrolidine (8)

To a round bottom flask (100 mL) with a magnetic stir bar was added pyrrolidine (1 g, 14 mmol), THF (10 mL) and triethylamine (1.94 mL, 14 mmol). The mixture was cooled to 0 °C and benzyl bromide (1.67 mL, 21 mmol) was added drop-wise over 15 min. The mixture was stirred until all the substrate was consumed. The solids were filtered and the filtrate was concentrated *in vacuo*. The crude product **8** was dissolved in CH_2Cl_2 (2 mL) and washed with water (2 mL). The organic phase was dried with $MgSO_4$, filtered and concentrated giving **8** (1.0 g, 46%) as yellow oil [27].

^{1}H NMR (400 MHz, $CDCl_3$): δ 1.81 ppm (m, 4H, CH_2), 2.53 (m, 4H, CH_2), 3.64 (s, 2H, CH_2), 7.31 (m, 5H, Ph). ^{13}C NMR (100 MHz, $CDCl_3$): δ 23.5 ppm, 54.3, 60.9, 126.9, 128.3, 129.0, 139.5.

3. Results and discussion

3.1. Chemistry

In the case of the synthesis of 1-benzyl-3-hydroxypyrrolidine derivatives [22] D- or L-malic acid were used as substrates (Scheme 1). In the case of compounds **1** and **1′**, two methods were used, in the first method only 89% ee was obtained (1st step formation of hydroxyamide; 2nd step cyclization to form the malimide). The first method was originally reported by Bhat et al. [22b]. It seems that the second step which involved heating at high temperature without solvent gave some racemization. In the second method using a direct thermally induced condensation between the malic acid and the amine, in xylene, an enantiopurity of 99% ee was obtained. For the synthesis of **3** and **3′** the method described by Zheng et al. [22a], was used and the yields were approximately 50%. The acetylation of **1**, **1′**, **3**, and **3′** with pyridine and acetic anhydride formed the products **2**, **2′**, **4** and **4′**, respectively [7].

The non-hydroxylated 1-benzyl pyrrolidine **8** was synthesized by alkylation of pyrrolidine using triethylamine and benzyl bromide, furnishing the product in a yield of 46% without any purification (Scheme 2). This compound was used as a reference. (3*R*,4*R*)-1-Benzyl-3,4-pyrrolidinediol **5** and the respective enantiomer **5′** were synthetized using the method of Nagel [23]. The dibenzylated derivative **6** was obtained by protecting the hydroxyl groups of **5** using NaH in DMF and benzylbromide, the yield was good.

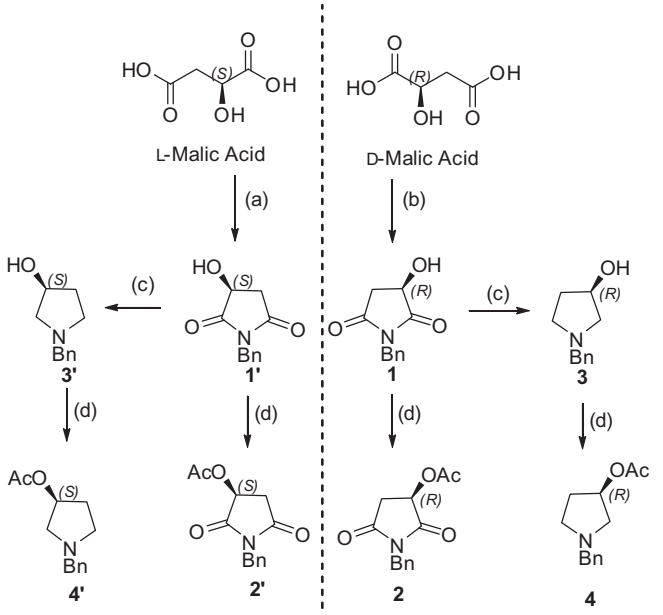

Scheme 1. *Reaction conditions*: (a) (i) $BnNH_2$, $MeOH/H_2O$, 170 °C; (ii) 160 °C (b) $BnNH_2$, Xylene, 170 °C (c) $LiAlH_4$, THF, NaOH (20%) (d) py, Ac_2O, rt.

(3*R*,4*R*)-Pyrrolidine-3,4-diol **7** (Scheme 3) was synthetized using supported palladium (0) – Pd-EnCat – and this was used in order to avoid leaching of the metal into the product, which is a problem with these systems [28].

3.2. Biological screening and toxicological studies

The synthetized compounds were assayed for the inhibition of rat intestine α-glucosidase using inhibitor concentrations between 0 and 46 mM, with the exception of compound **8** which was used at concentrations of 0 and 92 mM. DNJ was used as the positive control. The IC_{50} for DNJ inhibition of rat α-glucosidase was found to be in the nM range (IC_{50} = 0.167 ± 0.016 μM) (Fig. 3(A)) and consistent with other reports [29]. Table 1 shows the IC_{50} of the studied iminosugars, determined by the inhibition curves (Fig. 4(A)). Based on the results shown in Table 1, all the compounds containing a 2,5-carbonyl group (**1**, **1′**, **2**, **2′**) failed to evoke any inhibition; on the contrary all the examples lacking this group have shown inhibition in the concentration range 0.01–72 mM. As expected 1-benzylpyrrolidine **8**, showed very poor inhibitory action (with an IC_{50} of 72 mM), suggesting the requirement of hydroxyl groups in the pyrrolidine ring. Both enantiomers **2** and **2′**, have an acetoxyl group in the 3-position of the pyrrolidine ring. In this case, however, it was not possible to determine an exact IC_{50} value; instead a value in the range of 10–20 mM was inferred. The main reason for this result was that probably the acetylated compounds suffered partial hydrolysis during the inhibition period leading to a mixture of acetylated and deacetylated products. In the case of the monohydroxylated compounds **3** and **3′**, the IC_{50}'s were 4.6 ± 0.1 and 4.2 ± 0.3 mM, respectively. These compounds are

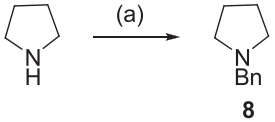

Scheme 2. *Reaction conditions*: (a) NEt_3, THF, BnBr, 0 °C to rt.

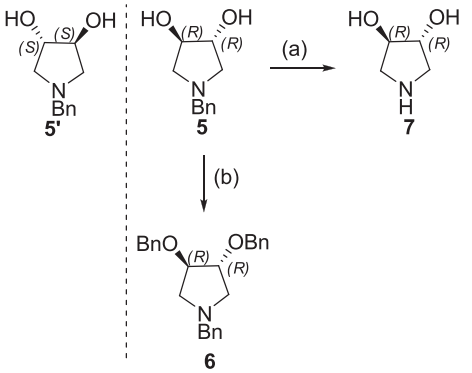

Scheme 3. *Reaction conditions*: (a) Pd(0)EnCat, EtOH, H_2; and (b) NaH, DMF, BnBr.

Table 1
The concentrations of iminosugar giving 50% inhibition of α-glucosidase from rat intestine mucosa.

Inhibitor	IC_{50} (mM)
DNJ	$1.67 \times 10^{-4} \pm 0.163 \times 10^{-4}$
1	NI
1′	NI
2	NI
2′	NI
3	4.6 ± 0.1
3′	4.2 ± 0.3
4	10–20
4′	10–20
5	2.97 ± 0.046 (K_I = 1.18 mM)
5′	5.82 ± 0.034 (K_I = 0.27 ± 0.25 mM) 0.01 ± 0.015
6	7.94
7	4.07 ± 0.042 (K_I = 0.44 ± 0.164 mM)
8	72.0 ± 0.3

NI: no inhibition.

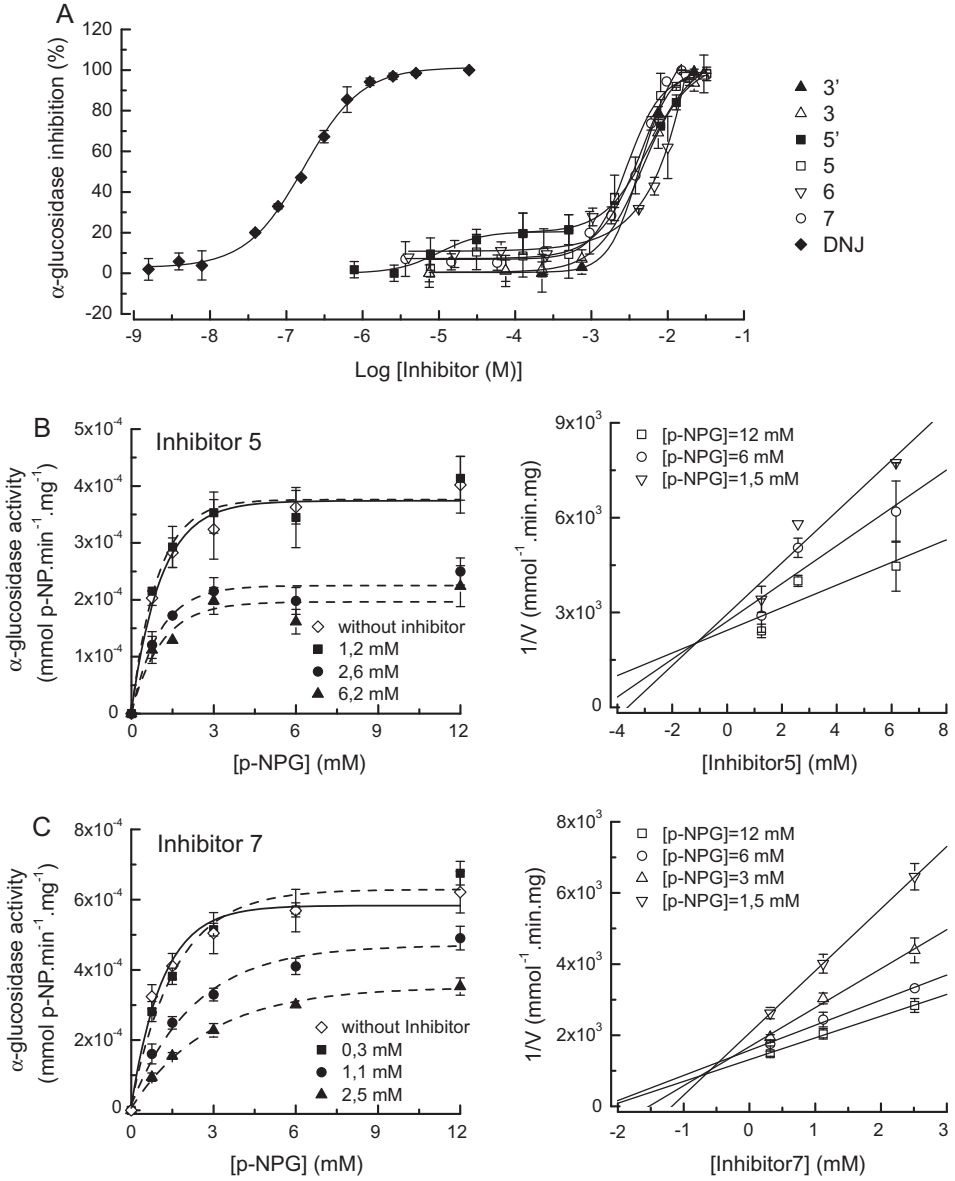

Fig. 4. (A) Inhibitory effects of compounds DNJ (♦), 3 (△), 3′ (▲), 5 (□), 5′ (■), 6 (▽) and 7 (○) against rat α-glucosidase activity, using *p*-nitrophenol-α-D-glucopyranoside as a substrate. Values are expressed as the mean ± sd (obtained in two independent experiments performed in quintuplicate). DNJ served as positive control. (B) Michaelis–Menten Plot and Dixon Plot for compound **5** in the presence of several concentrations for determination of K_I. (C). Michaelis–Menten plot and Dixon plot for compound **7** in the presence of several concentrations for determination of K_I. The values are expressed as mean ± sd (5 replicates).

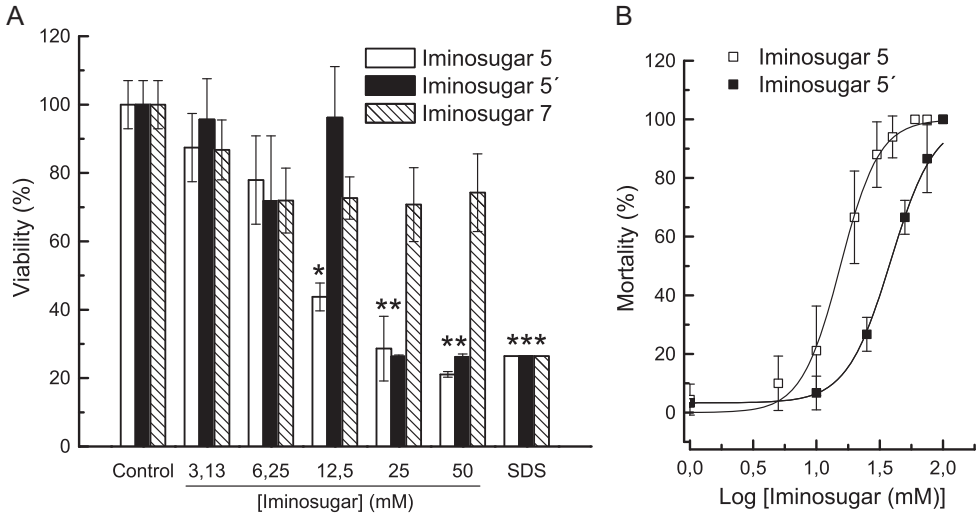

Fig. 5. (A) Viability of BRIN BD-11 cells with different concentrations of compounds **5**, **5′** and **7**. Batches of cells without inhibitors (control) and with 1% SDS, a cell membrane disrupter, were used as negative and positive controls, respectively. *Indicates statistical significance relative to controls ($p < 0.05$). (B) Mortality (%) of *artemia salina* vs log[iminosugar **5** or **5′**] – dose–response curve.

better inhibitors than the respective acetylated compounds (**2** and **2′**), perhaps as a result of better interactions with the active site of the enzyme. The same was the case for compound **6**, with a lower IC_{50} value compared to that of compound **5**. Another problem with compound **6** was its poor solubility in the assay solution hence deviations in the solution concentration might occur. In the case of the enantiomers **5** and **5′**, the IC_{50} values were 2.97 ± 0.046 and 5.82 ± 0.034 mM, respectively. Interestingly **5** is more active than **5′**. In an attempt to achieve better inhibition we decided to synthesize compound **7**, based on the modification of the structure of enantiomer **5**, making it more polar, with a free NH group for interaction by hydrogen bonding, with the active site of the enzyme. Unfortunately, the IC_{50} values increased slightly to 4.07 ± 0.042 mM. On comparing the monohydroxyl with the dihydroxyl compound series, the inhibition is quite similar. Based on these results, our best inhibitor was compound **5**.

In order to understand the molecular interactions between the inhibitors and the enzyme, we carried out some kinetic studies basically to determine the type of inhibition and the (K_I) value Fig. 4 and Table 1.

Only three compounds were selected, **5**, **5′** and **7**, which were the most promising inhibitors. On the basis of the kinetic results, all the compounds showed a mixed type of inhibition (Fig. 4(B) and (C)). Based on the Dixon plot, the mechanism of inhibition observed is predominately a mixed competitive type. The K_I values that were determined were different from the respective IC_{50} values, again indicating competitive inhibition.

Despite the fact that these compounds were moderate α-glucosidase inhibitors, it still was considered of interest to evaluate their toxicological proprieties, particularly as they could be used to address other therapeutic targets. The methods used were (i) BRIN-BD11 cell viability assay and (ii) *artemia Salina* toxicity assay. In the case of the first method used, Fig. 5(A), it was observed that compounds **5**, **5′** and **7** had low toxicity, compound **5** is the most toxic affecting the cellular viability for concentrations above 12.5 mM and compound **5′** affected the cellular viability for concentrations above 25 mM whereas **7** did not affect the cellular viability in the range of concentrations studied, up to 50 mM. It is noteworthy that these concentration values are 4 and 10 times higher than the IC_{50} of compounds **5**/**5′** and **7**, respectively. In the case of the tests with *artemia salina* only the enantiomers **5** and **5′** were evaluated. The results obtained show that the LC_{50} values were 15.53 and 38.56 mM, respectively (Fig. 5(B)). For both compounds the LC_{50} is 5 times higher than the IC_{50}. These results are in agreement with the cellular viability test and show that **5′** is less toxic than **5**. These results suggest that, although moderate inhibitors of mammalian α-glucosidase were used, these compounds might have some potential as pharmacological agents for other therapeutic targets. In addition, enantiomers **5** and **5′** are more toxic than compound **7**, suggesting that benzylated pyrrolidines are more deleterious than debenzylated ones.

3.3. Molecular modeling studies

In order to rationalize the experimental inhibitory activity for the compounds with different types of substitution in positions 2–5, the compounds were docked into the two enzymes active site. All the compounds were protonated when docked at the α-glucosidase active site. The results obtained for both enzymes were very similar, thus for simplicity, only the docking results using human α-glucosidase will be discussed.

As stated in our previous paper, the docking results show that all the tested compounds occupy the same region of the binding pocket as the amino group and the corresponding cyclohexenyl ring of acarbose. The obtained docking poses show all the compounds lying inside the binding cavity and interacting with the most important residues, notably, Asp203, Asp542, Asp443, Asp327 Arg526 and His600. We also docked DNJ into the α-glucosidase active site and this showed that the most active compounds show a very similar pose when compared with the ones obtained for DNJ (Fig. 3).

Compound **5**, the most potent compound in the series, is predicted to form an H-bond between the pyrrolidine nitrogen and Asp443 (1.5 Å), as well as having interactions between the oxygen atoms from the free hydroxyl groups, with Asp327, Asp542 and His600 (catalytic site) stabilizing the enzyme ligand complex, in a similar fashion to acarbose and DNJ. A very similar pose is observed for compound **7**, however, contrary to the former, this compound cannot establish interactions with Asp203 due to lack of the N-benzyl group. Compounds **3**, **3′**, **6** and **8** show an inverted pose inside the binding pocket compared with compounds **5** and **7**. However, it was shown that they can establish key interactions with Asp203, Arg526 and Asp542. When we compare, for example compounds **5** and **3** we observed an opposite orientation (pose)

inside the binding cavity, bearing testimony to the importance of disubstitution for stabilizing interactions that can improve inhibitory activity. Compounds **1**, **1′**, **2** and **2′** showed a rotated pose (~90°) inside the binding pocket when compared with compound **5**. Despite the fact, that these compounds occupy the same region as the active ones, their lack of activity might be due to the fact that they have carbonylic oxygen H-bond acceptors at positions 2 and 5, apparently forcing them to rotate and lose the important H-bonding interaction with Asp542.

4. Conclusions

Compounds with carbonyl groups in the 2,5-positions of the pyrrolidine ring did not show any α-glucosidase inhibition. Compounds with protected hydroxyl groups and without this group were shown to be poor inhibitors.

On comparing 3-hydroxypyrrolidine with (3,4)-dihydroxypyrrolidine, equivalent IC_{50} values were observed. However, compound **5**, a (3*R*,4*R*)-dihydroxypyrrolidine, was the best inhibitor with a IC_{50} value of 2.97 ± 0.046 mM. Compound **5** was more potent than its respective enantiomer.

Kinetic studies on compounds **5**, **5′** and **7** revealed a mechanism of inhibition predominantely of the mixed competitive type. Toxicological evaluation has shown that the compounds studied have, in general, low toxicity, only presenting deleterious effects for concentrations that are 4–10 times higher than the IC_{50}. Finally, the *N*-benzylated compounds are more toxic than the debenzylated compound **7**.

Our docking studies suggest that a rotation of ~90° of some compounds inside the binding pocket is responsible for the complete loss of inhibitory activity.

We are currently looking at the synthesis of libraries of novel sugar-pyrrolidine-diols for glucosidase inhibition as well as other activities.

Acknowledgments

EPC thanks the Fundação para a Ciência e a Tecnologia (FCT) for a post-doctoral research fellowship (SFRH/BPD/72182/2010). We are very grateful to Dr. Olivia Furtado Burke of LNEG, Lisbon for the optical activity measurements. We acknowledge LabRMN at FCT-UNL for the acquisition of the NMR spectra; the NMR spectrometers are part of the National NMR Network and currently supported by the FCT (RECI/BBB-BQB/0230/2012). We are grateful also from funding from FCT via the Strategic Projects PEst-OE/QUI/UI0619/2011. PEst-C/SAU/LA0001/2011 (CNC), PEst-OE/SAU/UI4013/2014 and PEst-C/QUI/UI0062/2011 (ICAAM). The University of Vigo (Spain) is gratefully acknowledged for MS analysis.

Appendix A. Supplementary material

Supplementary data associated with this article can be found, in the online version, at http://dx.doi.org/10.1016/j.bioorg.2014.04.007.

References

[1] (a) V.H. Lillelund, H.H. Jensen, X. Liang, M. Bols, Chem. Rev. 102 (2002) 515;
(b) M. Sugiyama, Z. Hong, P.-H. Liang, S.M. Dean, L.J. Whalen, W.A. Greenberg, C-H. Wong, J. Am. Chem. Soc. 129 (2007) 14811–14817. and references cited therein.
[2] (a) N. Zitmann, A.S. Metha, S. Carroueé, T.D. Butters, F.M. Platt, J. McCauley, B.S. Blumberg, R.A. Dwek, T.M. Block, Proc. Natl. Acad. Sci. USA 96 (1999) 11878–11882;
(b) N.J. Asano, J. Enzyme Inhib. 15 (2000) 215–234.
[3] (a) A. Mitrakou, N. Tountas, A.E. Raptis, R.J. Bauer, H. Schulz, S.A. Raptis, Diab. Med. 15 (1998) 657–660;
(b) A. Trapero, A. Llebaria, J. Med. Chem. 55 (2012) 10345–10346.
[4] J.R. Jacob, K. Mansfield, J.E. You, B.E. Tennant, Y.H. Kim, J. Microbiol. 45 (2007) 431–440.
[5] G.S. Jacob, Curr. Opin. Struct. Biol. 5 (1995) 605–611.
[6] T. Butters, R.A. Dwek, F.M. Platt, Curr. Top. Med. Chem. 3 (2003) 561–574.
[7] (a) L.R. Guerreiro, E.P. Carreiro, L. Fernandes, T.A.F. Cardote, R. Moreira, A.T. Caldeira, R.M. Guedes, A.J. Burke, Bioorg. Med. Chem. 21 (2013) 1911–1917. and references cited therein;
(b) N.S.H.N. Moorthy, N.F. Bras, M.J. Ramos, Bioorg. Med. Chem. 20 (2012) 6945;
(c) C. Bello, M. Cea, G. Dal Bello, A. Garuti, I. Rocco, G. Cirmena, E. Moran, A. Nahimana, M.A. Duchosal, F. Fruscione, P. Pronzato, F. Grossi, F. Patrone, A. Ballestrero, M. Dupuis, B. Sordat, A. Nencioni, P. Vogel, Bioorg. Med. Chem. 18 (2010) 3320;
(d) E. Moreno-Clavijo, A.T. Carmona, Y. Vera-Ayoso, A.J. Moreno-Vargas, C. Bello, P. Vogel, I. Robina, Org. Biomol. Chem. 7 (2009) 1192.
[8] M.L. Sinnott, Chem. Rev. 90 (1990) 1171–1202. and references cited therein.
[9] (a) G.W.J. Fleet, S.J. Nicholas, P.W. Smith, S.V. Evans, L.E. Fellows, R.J. Nash, Tetrahedron Lett. 26 (1985) 3127–3130;
(b) A.M. Scofield, L.E. Fellows, R.J. Nash, G.W.J. Fleet, J. Life Sci. 39 (1986) 645–650;
(c) G.W.J. Fleet, P.W. Smith, Tetrahedron 42 (1986) 5685–5692;
(d) J.R. Behling, A.J. Campbell, K.A. Babiak, J.S. Ng, J. Medich, P. Farid, G.W.J. Fleet, Tetrahedron 49 (1993) 3359–3366.
[10] F.P. Cruz, S. Newberry, S.F. Jenkinson, M.R. Wormald, T.D. Butters, D.S. Alonzi, S. Nakagawa, F. Becq, C. Norez, R.J. Nash, A. Kato, G.W.J. Fleet, Tetrahedron Lett. 52 (2011) 219–223.
[11] (a) A. Kato, E. Hayashi, S. Miyauchi, I. Adachi, T. Imahori, Y. Natori, Y. Yoshimura, R.J. Nash, H. Shimaoka, I. Nakagome, J. Koseki, S. Hirono, H. Takahata, J. Med. Chem. 55 (2012) 10347–10362;
(b) T.M. Chapman, S. Courtney, P. Hay, B.G. Davis, Chem. Eur. J. 9 (2003) 3397. and references cited therein.
[12] E.-L. Tsou, S.-Y. Chen, M.-H. Yang, S.-C. Wang, T.-R.R. Cheng, W.-C. Cheng, Bioorg. Med. Chem. 16 (2008) 10198–10204.
[13] (a) P.-H. Liang, W.-C. Cheng, Y.-L. Lee, H.-P. Yu, Y.-T. Wu, Y.-L. Lin, C.-H. Wong, Chem. BioChem. 7 (2006) 165;
(b) P.-H. Liang, Y.-L. Lin, C.-H. Wong, Patent Application US2012/0046337 A1 (2012).
[14] M. Takebayashi, S. Hiranuma, Y. Kanie, T. Kajimoto, O. Kanie, C.-H. Wong, J. Org. Chem. 64 (1999) 5280–5291.
[15] M. Bols, Tetrahedron Lett. 37 (1996) 2097–2100.
[16] M. Godskesen, I. Lundt, Tetrahedron Lett. 39 (1998) 5841–5844.
[17] (a) S.G. Pyne, M. Tang, Curr. Org. Chem. 9 (2005) 1393;
(b) K. Tamazawa, H. Arima, T. Kojima, Y. Isomura, M. Okada, S. Fujita, T. Furuya, T. Takenaka, O. Inagaki, M. Terai, J. Med. Chem. 29 (1986) 2504.
[18] W. Hakamata, M. Kurihara, H. Okuda, T. Nishio, T. Oku, Curr. Top. Med. Chem. 9 (2009) 3–12.
[19] (a) M. Watford, P.H. Lund, Biochem. J. 178 (1979) 589–596;
(b) M.M. Bradford, Anal. Biochem. 72 (1976) 248–254.
[20] (a) G. Jones, P. Willett, R. C. Glen, J. Mol. Biol., 1995, vol. 245, pp. 43–53.; G. Jones, P. Willett, R.C. Glen, A.R. Leach, R. Taylor, J. Mol. Biol., 1997, vol. 267, pp. 727–748.;
(b) GoldScore performs a force field based scoring function and is made up of four components: (1) Protein-ligand hydrogen bond energy (external H-bond); (2) Protein-ligand van der Waals energy (external vdw); (3) Ligand internal van der Waals energy (internal vdw); (4) Ligand intramolecular hydrogen bond energy (internal-H-bond).
[21] L. Sim, K. Jayakanthan, S. Mohan, R. Nasi, B.D. Johnston, B. Mario Pinto, D.R. Rose, Biochemistry 49 (2010) 443–451.
[22] (a) J.-L. Zheng, H. Liu, Y.-F. Zhang, W. Zhao, J.-S. Tong, Y.-P. Ruan, P.-Q. Huang, Tetrahedron: Asymm. 22 (2011) 257–263;
(b) K.L. Bhat, D.M. Flanagan, M.M. Joullié, Synth. Commun. 15 (1985) 587–598.
[23] (a) U. Nagel, E. Kinzel, J. Andrade, G. Prescher, Chem. Ber. 119 (1986) 3326;
(b) W. Beck, U. Nagel, 1985, US patent, 4,634,775.
[24] A. Naylor, D.B. Judd, D.I.C. Scopes, A.G. Hayes, P.J. Birch, J. Med. Chem. 37 (1994) 2138–2144.
[25] P.D. Cesare, D. Bouzard, M. Essiz, J.P. Jacquet, B. Ledoussal, J.R. Kiechel, Remuzon, R.E. Kessler, J. Fung-Tomc, J. Desiderio J. Med. Chem. 35 (1992) 4205–4213.
[26] H. Tomori, K. Shibutani, K. Ogura, Bull. Chem. Soc. Jpn. 69 (1996) 207–215.
[27] J.R. Sundberg, C.P. Walters, J.D. Bloom, J. Org. Chem. 46 (1981) 3730–3732.
[28] (a) J. Toubiana, M. Chidambaram, A. Santo, Y. Sasson, Adv. Synth. Catal. 350 (2008) 1230–1234;
(b) http://reaxa.com/applications_Encat_30NP.html (29.09.13).
[29] C. Kuriyama, O. Kamiyama, K. Ikeda, F. Sanae, A. Kato, I. Adachi, T. Imahori, H. Takahata, T. Okamoto, N. Asano, Bioorg. Med. Chem. 16 (2008) 7330–7336.